

Effects of Decaying Image Currents on
Electron Rings During Compression Between
Side Walls and Motion Along Conducting
Cylinders ⁺

W.Herrmann

IPP 0/25

Nov.1974

MAX-PLANCK-INSTITUT FÜR PLASMAPHYSIK

GARCHING BEI MÜNCHEN

MAX-PLANCK-INSTITUT FÜR PLASMAPHYSIK
GARCHING BEI MÜNCHEN

Effects of Decaying Image Currents on
Electron Rings During Compression Between
Side Walls and Motion Along Conducting
Cylinders ⁺

W.Herrmann

IPP 0/25

Nov.1974

*Die nachstehende Arbeit wurde im Rahmen des Vertrages zwischen dem
Max-Planck-Institut für Plasmaphysik und der Europäischen Atomgemeinschaft über die
Zusammenarbeit auf dem Gebiete der Plasmaphysik durchgeführt.*

Effects of Decaying Image
Currents on Electron Rings
During Compression Between
Side Walls and Motion Along
CylindersAbstract

Decaying image currents consume energy which has to be supplied by the field producing electron ring. For very high currents ($I > 10^3$ A, particle number $N_e \approx 10^{14}$) the losses become important and have to be included in the calculation of the ring dynamics. Special attention has been given to the focussing effects of the decaying image currents during compression and to the retarding force which develops when the ring is moved along a resistive cylinder. It is emphasized that in the latter case the ring experiences a "run-away-situation", when the ratio of its velocity to the surface resistivity exceeds a certain limit.

A Introduction

Magnetic fields set up in the neighborhood of conducting walls induce eddy currents, which owing to the finite resistivity of the walls lead to energy losses. In ¹ these losses were calculated for cylindrical geometry in the case of a sudden increase in the field, such as occurs during the formation of an electron ring in the electron ring accelerator. If the rise time of the self-field of the ring is shorter than the penetration time through the walls, the results of ¹ can be applied. The amount of energy dissipated during the penetration process is less than 1% of the ring kinetic energy for the known compressors, as long as the particle number is less than 10^{13} . For 10^{14} electrons the energy loss, which has to be supplied from the energy of the injected electrons, is pronounced. Considering this effect, the question arose whether the energy loss during the compression between side walls or during roll-out along conducting cylinders is also of the order, and whether its effect has to be taken into account in calculating the ring dynamics.

This question shall be answered in this report for the two separate cases which correspond to radial compression and axial roll-out in electron ring accelerators. The program used for this calculation is an extended version of the one described in ¹. It is capable to compute the effects of a ring moving close to resistive structures, as long as the system is axisymmetric. The problem is not solved self-consistently; the motion of the ring is prescribed. Effects of resistive wall instabilities exceed the scope of this report.

In the course of the calculation it turned out that the influence of the image currents on focussing and acceleration might be much more important than the energy loss. Much more attention has therefore been given to these problems. A paper of P. Merkel ² deals with the motion of a linear beam along conducting walls of arbitrary thickness and gives an analytical solution in linear geometry. In section D a short comparison is made between the two calculations.

Section B describes the computational procedure and states its limits of validity. In section C the case of the compression of a ring between side walls onto a cylinder is treated and special attention is given to the effects of focussing. Section D deals with the motion of a ring along a cylinder and here the main interest is focussed on the retarding power originating from the decaying image currents. Beyond a certain velocity of the ring a situation develops, where it is almost impossible in practical situations to control the acceleration of the ring. The term "run-away-situation" is used to describe this behaviour of the ring. It is of great importance, to know, how this situation can be avoided.

B Computational Procedure

The computation is done for axisymmetric geometry. The walls are supposed to be thin sheets with thicknesses small compared to the skin depths in question. The current density across the thickness of the walls is therefore assumed to be constant. The assumption that the skin depth is larger than the wall thickness is correct, as long as the DC surface resistivity is $s [\Omega/\square] \geq 2,4 \cdot 10^{-5} \left(\frac{\rho g}{d}\right)^{1/2}$.

Here v is the velocity of the ring parallel to the wall (radial or axial) in [cm/sec], ρ the resistivity in [Ω mm] and d the distance of the ring from the wall in [cm]. For silver coatings and velocities of $v = 10^6$ [cm/sec] and $d = 0.5$ [cm] s would have to be larger than 0.13 [$m\Omega/\square$].

The walls are subdivided into flat cylindrical elements numbered by n . The n -th element is assigned a self-inductance L_{nn} and a resistance R_n . The elements are interconnected and coupled to the ring through mutual inductances M_{nm} . The following formulas³ are used for L, M and R:

$$L_{nn} = \mu_0 \cdot r_n \cdot \left(\ln \frac{8 r_n}{D_n} - 0.5 \right)$$

$$M_{nm} = \mu_0 \sqrt{r_n \cdot r_m} \cdot \left(\left(\frac{2}{k} - k \right) \cdot K - \frac{2}{k} \cdot E \right)$$

$$k = 2 \cdot \left(r_n \cdot r_m / \left((r_n + r_m)^2 + (z_n - z_m)^2 \right) \right)^{1/2}$$

$$R_n = 2 \pi r_n \cdot s_n / D_n$$

Here r_n is the central radius and z_n the axial position of the n -th element and D_n its width. K and E are the elliptic integrals of the first and second kinds and k their argument.

To get the time behaviour of the induced eddy currents in the elements, one has to solve the following system of equations:

$$\sum_{m=1}^N L_{nm} \dot{I}_m = -R_n I_n - \frac{d}{dt} (M_{nR} I_R) \quad n=1, \dots, N \quad (1)$$

M_{nR} is the mutual inductance between the ring and the n -th element. N is the number of elements. The system was solved for I_n with the help of the matrix inversion program MINV, supplied by IBM, and the currents as a function of time were obtained by means of HPCG, a predictor-corrector method, also supplied by IBM.

The driving term on the right-hand side $\frac{d}{dt} (M_{nR} I_R)$, allowed for changes in ring current I_R as well as changes in geometry. For simplicity the ring velocity was always assumed to be constant. Two special cases were considered:

1.) Compression of a ring between conducting side walls. Two sub-cases have been calculated. The first one assumed, that the ring has been formed a long time before the compression starts, such that the ring selffields already had penetrated the walls at the beginning of compression. The second case starts with the buildup of the ring current and performs compression immediately thereafter. The process of ring formation is assumed to be that fast, that almost no resistive energy loss occurs during formation time.

2.) Motion of a ring along a cylinder.

In all calculated cases s_n was the same for all elements for reasons of simplicity. Then eq.1 can be divided by $s = s_n$ and t replaced by $\tau = s \cdot t$. The time derivative in the driving term is expressed by the following relations for the radial or axial motions respectively:

$$\frac{d}{d\tau} = \frac{v}{S} \cdot \frac{d}{dr} \quad , \quad \frac{d}{dz} = \frac{v}{S} \cdot \frac{d}{dz}$$

The currents in the wall depend on v and S as a function of τ only in the form v/S . The energy loss E_L during the time T is given by:

$$E_L = \int_0^T \sum_N R_N \cdot I_N^2 dt$$

With $R_N = \alpha_N \cdot S$; $\tau_N = S_N \cdot T$ and α_N a function of geometry only one gets

$$E_L = \int_0^{\tau_1} \sum_N \alpha_N I_N^2 d\tau$$

For unit distance of ring motion one has: $\tau_1 = \frac{S}{v}$. It follows that the energy loss per unit distance of ring motion for the same geometry and constant ring current depends on the ratio of S and v only. In addition it can be shown that the results are the same as long as the geometries are similar.

Fortunately, the full set of equations had to be solved in a limited regime of v/S only. For large v/S as well as for small v/S simple approximations are valid. For large v/S the term $R_N I_N$ is small compared to $\frac{d}{d\tau}(M_{NR} I_R)$. In this case the currents can be obtained by simple integration after the inversion of the matrix. The current distributions are then independent of the resistivity and the ring velocity, but the energy loss per cm is inversely proportional to v/S . In the case of high wall resistivity the currents in the elements are determined by the driving term and the resistivity, and the left-hand side of eq.1 can be neglected. The currents are then proportional to the velocity of the ring and inversely proportional to the resistivity. The energy loss per unit distance of ring motion in this case is proportional to v/S . In between these two limiting cases the full set of equations has to be solved.

C Compression Between Side Walls

In the case of radial compression of a current carrying ring of electrons between conducting side walls both the energy loss and

the focussing force depend very much on the specific geometry. The cases described here may be taken as a paradigm showing the order of magnitude of the expected effect. The geometry underlying the calculations described here, is the following: Two parallel side plates are at a distance of 5 cm from each other. The ring is compressed in the midplane between the plates. They have a major radius of 27 cm and a hole on axis with a radius of 3 cm. Along the axis there is a cylinder with a radius of 2 cm and extending ± 3.2 cm in the axial direction. In most of the calculations this cylinder was present because it was anticipated that it is present in all experiments for suppressing negative mass effects. The ring with a current of initially 1 A is compressed from 14 cm to 2.5 cm. The current in the ring increases inversely with the radius. At the position of the ring an axial magnetic field is assumed which corresponds to an energy of 2 MeV at $R = 14$ cm and increases inversely with the square of the radial ring position as is exact in a uniform field. For the calculation of the field index due to the image currents it was assumed that the axial field produced by the image currents is negligible compared with the main magnetic field. The resulting error in the field index is less than 5% for injected currents of up to 1000 A.

Fig.1 shows the absolute energy loss divided by the square of the initial ring current I_0 as a function of v/s . In Fig.2 this energy loss is related to the kinetic energy E_{kin} in the ring for an injected beam with 2 MeV in the following manner:

$$E_{rel} = \int_0^{T_e} \frac{dE_i/dt}{E_{kin}} dt = \int_{R_0}^{R_e} \frac{dE_i/dR}{E_{kin}} dR$$

T_e and R_e are the time and the radius at the end of compression respectively. This evaluation takes into account that the energy gain during compression is proportional to the energy at the beginning (for the same fields). That is, if the ring loses a certain percentage of its energy at a certain time, the subsequent energy gain by the compression is reduced by the same percentage.

The dashed curves in Fig.1 and 2 belong to the case without injection, the full curves represent the case with injection. The

curves numbered 1 give the integrated resistive losses at the end of compression. The curves numbered 2 give the energy, stored in the field of the wall currents at the end of compression. This energy is finally dissipated, if the ring stays long enough in the compressed state. The curves numbered 3 give the sum of 1 and 2. Fig.2 contains the same information for the relative losses.

In the case without inflection the losses up to the end of compression (curve 1) tend towards zero for very low and very high v/s . The two straight lines are the result of the approximate solution of eq.1 mentioned in section B. At the v/s -value for their intersection point curve 1 reaches a maximum. The energy stored in the field of the wall currents at the end of compression reaches a maximum for large v/s (curve 2) and so does the sum of dissipated and stored energy (curve 3).

The solid curves for the case with injection show a different behaviour. The actual losses at the end of compression go to zero for high v/s , but tend towards a finite value at low v/s . This value for low v/s corresponds to the losses connected with the penetration of the fields after injection without compression. The total losses due to compression (curve 3 dashed) are almost additive to the injection loss.

The maximum energy loss is about $2 \cdot 10^{-7} [J]$ for 1 A of ring current, for $10^3 [A]$ one gets a loss of $0,2 [J]$. This amounts to about 4% of the kinetic energy of a trapped ring with a radius of 14 cm and an energy of $2 [MeV]$. The relative losses calculated as described earlier are seen on Fig.2. For low v/s the relative losses are about 2% for $10^3 [A]$. (It is assumed that the ring is injected with $2 [MeV]$ at $R = 14 [cm]$) The total losses with injection reach a flat maximum at about $5 \times 10^7 [cm/sec/\Omega/D]$, and then decrease for increasing v/s . The relative losses due to compression only are negligible in most cases. Due to the fact that the compressing fields have to penetrate the side walls also, one will probably tend to work in the low v/s regime and has to face therefore mainly the losses connected with the rapid injection of the beam.

In the low v/s regime another effect can be important: As the image currents decay the image charges exert a force on the ring. For very good conductivity the forces of the image currents and the image charges almost cancel, if the ring is close to the walls. The force of the image charges after the decay of the currents is then the same but opposite in sign as the forces of the full image currents. The force itself leads to a change in the radius of the ring. This has not been calculated, since the radius of the ring is prescribed. But the derivative of the force influences the focussing of the ring. Fig.3 shows the change of the field index divided by the injected ring current $\Delta n/I_0$ at the ring position for the case that the image currents are absent. (This curve is calculated with injection at time zero.) A positive sign of $\Delta n/I_0$ means additional axial focussing and radial defocussing, a negative sign axial defocussing and radial focussing. The positive sign at the end of compression, when the ring is close to the cylinder on axis corresponds to the well-known effect of cylinders with axial conductivity only, the so-called squirrel cages⁴. Because the frequencies of the negative mass instability is so much higher than the frequency corresponding to the compression it is possible to choose a resistivity such, that a cylinder acts well conducting as far as the high frequencies of negative mass are concerned and bad conducting and therefore axially focussing for the low frequencies of compression.

For large ring radii Δn is negative, that is the side walls act axially defocussing. In order not to loose the ring integrity during compression, the Field index of the compressing field has to be kept so large, that the effect of the decaying image currents is compensated.

D Motion Along a Cylinder

The energy loss connected with the motion of a ring along a resistive cylinder can be of great importance when the ring has to be transported a long way very close to the surface. Fig.4 gives the

energy loss E_L normalized to the square of the current and the distance of the motion L for different ratios RV of the ring radius to cylinder radius. The calculation was done for sufficiently long cylinders, such that the end effects could be neglected. The normalized loss is independent of the radius of the ring as long as the ratio RV and the current are constant. For the same number of particles, however, and the same RV the losses are less, if the ring is on a larger radius. Also for the same distance of the ring from the cylinder the losses for large radii at constant current are larger than for small radii.

As in the radial compression case the losses go through a maximum as a function of v/s which shifts slightly to larger v/s for smaller RV . For 1500[A] in the ring at the end of compression the energy loss at the maximum for $RV = 0.8$ and a distance of motion of 30[cm] is 0.73[J], which corresponds to $\sim 7.3\%$ for a ring at a radius of 2.5[cm] and a kinetic energy of 13[MeV]. If the ring is moved at a v/s about an order of magnitude from the worst value, the energy losses are negligible in most cases, at least if one does not go to extremely high current. The straight lines in Fig.4 give the asymptotic behaviour for low and high v/s .

The linear calculation of ²⁾ fits rather well with the curve for $RV = 0.95$. For $RV = 0.8$ the linear calculation gives already a value 60% larger than the calculation for the cylindrical case.

For an infinitely long cylinder a stationary distribution of the image currents develops. As long as the resistivity is zero and the velocity unrelativistic, this distribution is symmetric around the z -position of the ring. For finite v/s the image currents decay and even change their sign behind the moving ring. The distribution is unsymmetric. At the position of the ring a radial magnetic field develops, which together with the azimuthal velocity of the ring electrons exerts a retarding force on the ring in axial direction. The scale at the right hand side of Fig.4 gives the radial magnetic field seen by the ring. (In the stationary state the retarding force equals the energy loss per cm. For finite length cylinders the radial magnetic field has to be cal-

culated from the current distribution.) Even for rings with moderate currents retarding fields can be produced, which are by far larger than the radial magnetic fields of a few Gauß, which can be applied in expansion acceleration in present day electron ring accelerators. For example with $1500[A]$, $RV = 0.8$ and a ring radius of $2.5[cm]$ the maximum retarding force corresponds to $B_r = 103[Gauß]$. This maximum occurs for values of $v/c \approx 2.25 \cdot 10^8 [cm/sec/\Omega]$. To accelerate a ring up to the peak velocity an external radial magnetic field (or corresponding electric field) larger than the one produced by the image currents is required. If the external field is less than the maximum image field the ring can only be accelerated to a velocity, at which the external field equals the retarding field. Because the retarding field depends on the current in the ring, the velocity to which a ring can be accelerated depends on the quality (current) of the ring for a given external field.

If the external field is larger than the peak retarding field and the ring is on the right hand side of the peak, the situation is even worse: If the ring gains velocity the retarding force is reduced. If the external field does not decrease rapidly enough in space the accelerating field - that is the difference between the external and the retarding field - on the ring gets the larger the faster the ring is. Fig.5 shows an example of the radial field seen by a ring, which moves along a cylinder in an external field composed by an homogeneous field in axial direction and a spatially constant radial field, which increases in time to finite values, above which it remains constant. The peak velocity is $2.25 \cdot 10^8$ cm/sec, the maximum retarding field $B_r = 112.5$ Gauß. If the external field reaches only values below the peak, the effective B_r seen by the ring stays small and goes to zero, when the external field got constant in time. But even if the external field is only slightly larger than the peak field, the radial field seen by the ring finally increases to very large values, which for the quality of the rings obtained so far, is far beyond the value, up to which ions would stay in the ring.

Although it seems possible to construct an external field such, that for certain conditions of the ring and the external field the acceleration stays inside the limits, posed by the achieved quality of the rings, small deviations from these conditions lead to uncontrollable accelerations. This situation on the large v/s side of the peak might be well described by calling it run-away-situation.

This run-away-effect does not allow to use conducting cylinders in the accelerating region of an electron ring accelerator - at least if high velocities should be obtained. In the roll-out phase these cylinders might be used, if v/s stays on the left hand side of the peak. But the rings have to cross the end of the cylinder slowly, to ensure that the retarding forces stay inside the limits. (For large v/s the end of a conducting cylinder - image charges neglected - acts accelerating for a certain distance, whereas for low v/s the force is always retarding. Calculations to the end effect shall be given in a separate report.)

If only velocities up to the value of v/s for the peak field are required and if the jitter in the velocity does not bother - this jitter in a typical example was of the same order as e.g. the jitter in ring current - conducting cylinders might be used. For a surface resistivity of $20 [\Omega/\square]$ axial velocities up to $4 \cdot 10^9$ [cm/sec] can be obtained. One has, however, to have in mind, that in this case a big fraction of the electron energy is lost to the walls and cannot be given to the ions.

E Summary and Discussion

For ring currents hitherto achieved energy losses of the induced image currents in resistive walls during compression seem to be unimportant. Only if the intended larger currents should be obtained, the losses have to be taken into account for the correct evaluation of the ring dynamics. During roll-out and acceleration it has to be ensured that the velocity is not for a long distance close to the value for the peak losses.

Important, however - even for moderate ring currents - appears to be the influence of the decay of the image currents on the focussing during radial compression. For a ring current of 400[A] ($7,5 \cdot 10^{12}$ electrons) and a realistic geometry as described in section C the effective field index n changes by $\Delta n = 0,12$, when the image currents fully decay. Resistive side walls act defocussing axially, a resistive cylinder focussing axially. Because of the big difference in frequency for the compression cycle and the electron revolution a resistive cylinder could be used for suppressing the negative mass instability as well as for providing axial focussing.

Even more important are retarding forces originating from the decaying image currents during roll-out and acceleration of the ring along resistive cylinders. The retarding forces in realistic cases can be much larger than the allowed effective accelerating forces. Beyond a certain speed the retarding forces decrease with increasing velocity, which provides a run-away-situation for the ring. This effect could be avoided if the desired velocity is below the critical one. This would be the case if v is kept below $4 \cdot 10^9$ [cm/sec] for surface resistivities of the cylinder of 20 [Ω]. In this case one has to live with a jitter in the obtained velocity, which is of the order of the jitter in the ring current.

Since the conducting structures are introduced to suppress the effects of the negative mass instability, the cylinder could be removed in the accelerating region only in such cases, where the negative mass instability is not considered to be serious. Under these circumstances the conducting cylinder could end in the neighbourhood of the spill-out point. One, however, has to ensure that the end of the cylinder is crossed with low speed because otherwise the image currents in the end produce a similar run-away effect.

The program as described in section B has been used to calculate two idealised examples. It is, however, capable to compute much more complicated systems as long as they are axially symmetric and the thickness of the walls does not exceed certain limits.

Acknowledgement

I am gratefully indebted to Dr. P. Merkel who directed my attention to the problem of the retarding forces. My thanks go to Prof. Schlüter and Dr. Merkel for helpful discussions.

References:

- 1) Frank Pohl
- 2) G.B. Dolbilov et al.

Fig. 2: Relative energy loss ϵ_{rel} divided by the injected current I_0 as a function of v/c . Otherwise the same as Fig. 1

Fig. 3: The difference in field index Δn at the ring position divided by the injected beam current I_0 as a function of radius R or time t for a compression velocity of $v/c = 10^{-2}$ (upper part) current with injection, dashed curve; lower part: Compression between 1.5 cm and 2.5 cm at a radius of 1 cm. Positive values are radially increasing, radially decreasing, negative values radially increasing, radially decreasing.

Fig. 4: Energy loss ϵ divided by the distance of motion L and the square of the ring current I^2 for the motion of the ring with a velocity v along a cylinder with a surface resistivity s as a function of v/c . R_c = cylinder radius to ring radius. The scale at the right side gives the radial magnetic field seen by a ring with radius R_c and current I due to the decaying image currents.

Fig. 5: Effective accelerating field B_{eff} as a function of time seen by a ring, which moves along a cylinder with $s = 1.0/c$ in a constant B_z -field, to which an increasing radial field constant in space is added. At certain levels, indicated at the curves, the radial field becomes constant in time.

References:

- 1.) W. Herrmann ERAN 197, Oct. 1972
- 2.) P. Merkel IPP O/24, Oct. 1974
- 3.) Frank Pohl IPP 1/57, Jan. 1967
- 4.) G.B. Dolbilov et al. JINR-P9-4737, Dubna (1969)

Figure Captions

- Fig.1: Energy loss E per injected current I_0^2 in Joule/A² as a function of the compression velocity v divided by the surface resistivity ζ of the sidewalls. Solid curves: with injection; dashed curves: without injection. Curves numbered 1: Energy lost during the compression. Curves numbered 2: Energy stored in the ^{field of the} wall currents at the end of compression. Curves numbered 3: the sum of curve 1 and 2. The straight dashed lines give the asymptotic behaviour for the dashed curve 1. The dotted line: estimate.
- Fig.2: Relative energy loss E_{rel} divided by the injected current I_0 as a function of v/ζ . Otherwise the same as Fig.1
- Fig.3: The difference in field index Δn at the ring position divided by the injected beam current I_0 as a function of radius R or time t for a compression velocity of $v_c = 10^6$ cm/sec. Full curve: with injection, dashed curve: without injection. Compression between 14 cm and 2,5 cm a cylinder at a radius of 2 cm. Positive values are axially defocussing, radially focussing, negative values axially focussing, radially defocussing.
- Fig.4: Energy loss E divided by the distance of motion L and the square of the ring current I^2 for the motion of the ring with a velocity v along a cylinder with a surface resistivity ζ as a function of v/ζ . $RV =$ cylinder radius to ring radius. The scale at the right side gives the radial magnetic field seen by a ring with radius R_{ring} and current I due to the decaying image currents.
- Fig.5: Effective accelerating field B_r as a function of time seen by a ring, which moves along a cylinder with $s = 1 - \Omega/\omega$ in a constant B_z -field, to which an increasing radial field constant in space is added. At certain levels, indicated at the curves, the ^{external} radial field becomes constant in time.

The maximum retarding field is 112.5 Gauß. For external fields below this value, the effective B_r at the ring stays rather low and goes to zero, when the external field got constant. If the external field is only slightly larger than the peak retarding field, the effective B_r at the ring finally increases almost up to the value of the external field.

Fig. 1: Energy loss E_{rel} as a function of v_{rel} . The dotted line is the asymptotic behaviour for the dashed curve 1. The dashed curve 2 and 3. The straight dashed lines give the asymptotic behaviour for the dashed curves 1, 2 and 3.

Fig. 2: Relative energy loss E_{rel} divided by the injected current I_0 as a function of v_{rel} . Otherwise the same as Fig. 1.

Fig. 3: The difference in field index Δn at the ring position divided by the injected beam current I_0 as a function of radius R or time t for a compressor velocity of $v_{rel} = 10^6$ cm/sec. Full curves: with injection, dashed curves: without injection. Compression between 14 cm and 2.5 cm; a cylinder at a radius of 5 cm; positive values are axially defocusing, negative values axially focussing.

Fig. 4: Energy loss E divided by the distance of motion L and the square of the ring current I_0^2 for the motion of the ring with a velocity v along a cylinder with a surface resistivity ξ as a function of v . $Rv = \text{cylinder radius} \times \text{ring radius}$. The scale at the right side gives the radial magnetic field seen by a ring with radius R and current I_0 due to the decaying image currents.

Fig. 5: Effective accelerating field E_{eff} as a function of time seen by a ring, which moves along a cylinder with $\alpha = 1 - Q/D$ in a constant B_z -field, to which an increasing radial field constant in space is added. At certain levels, indicated at the curves, the radial field becomes constant in time.

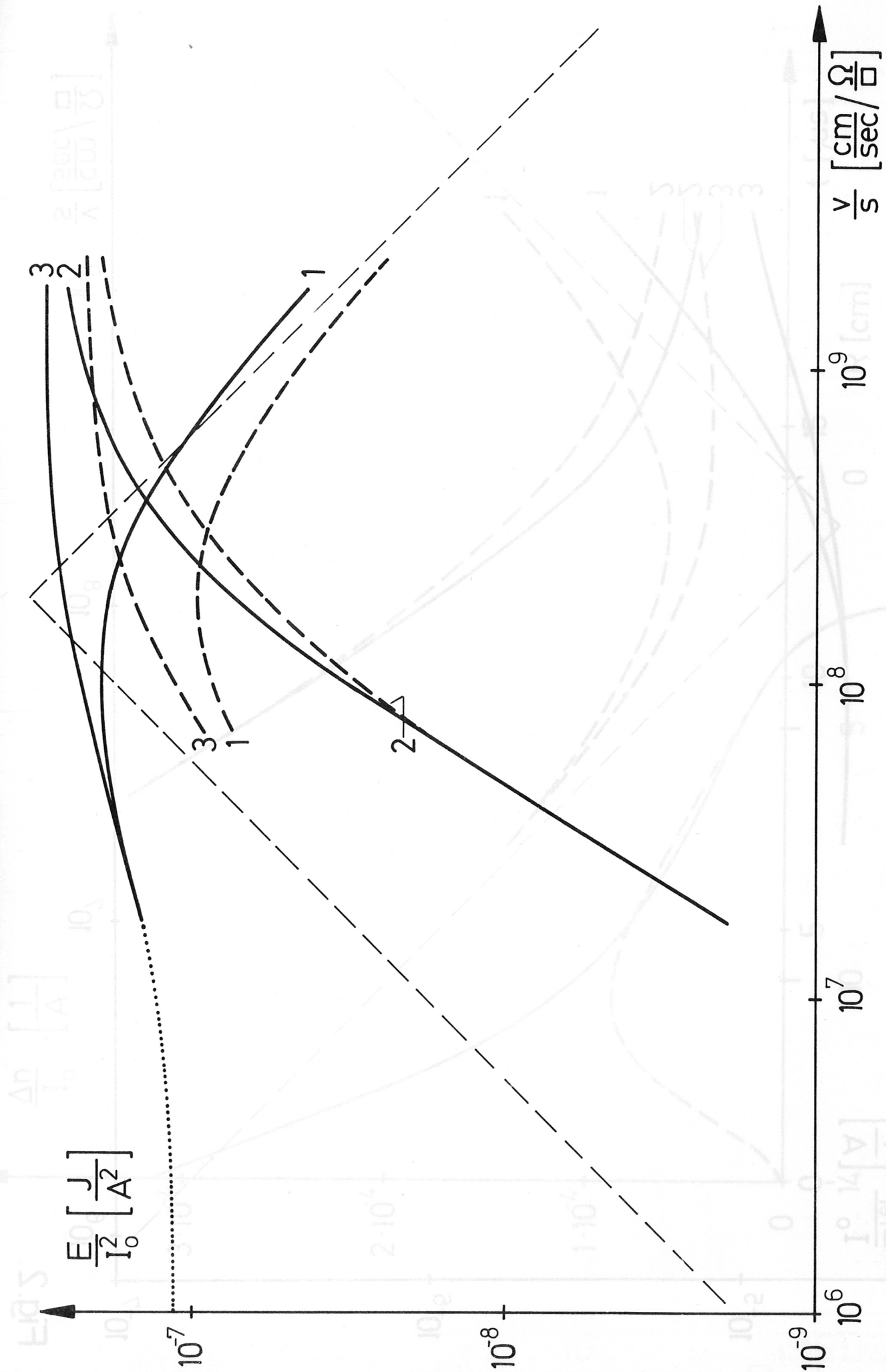


Fig. 1

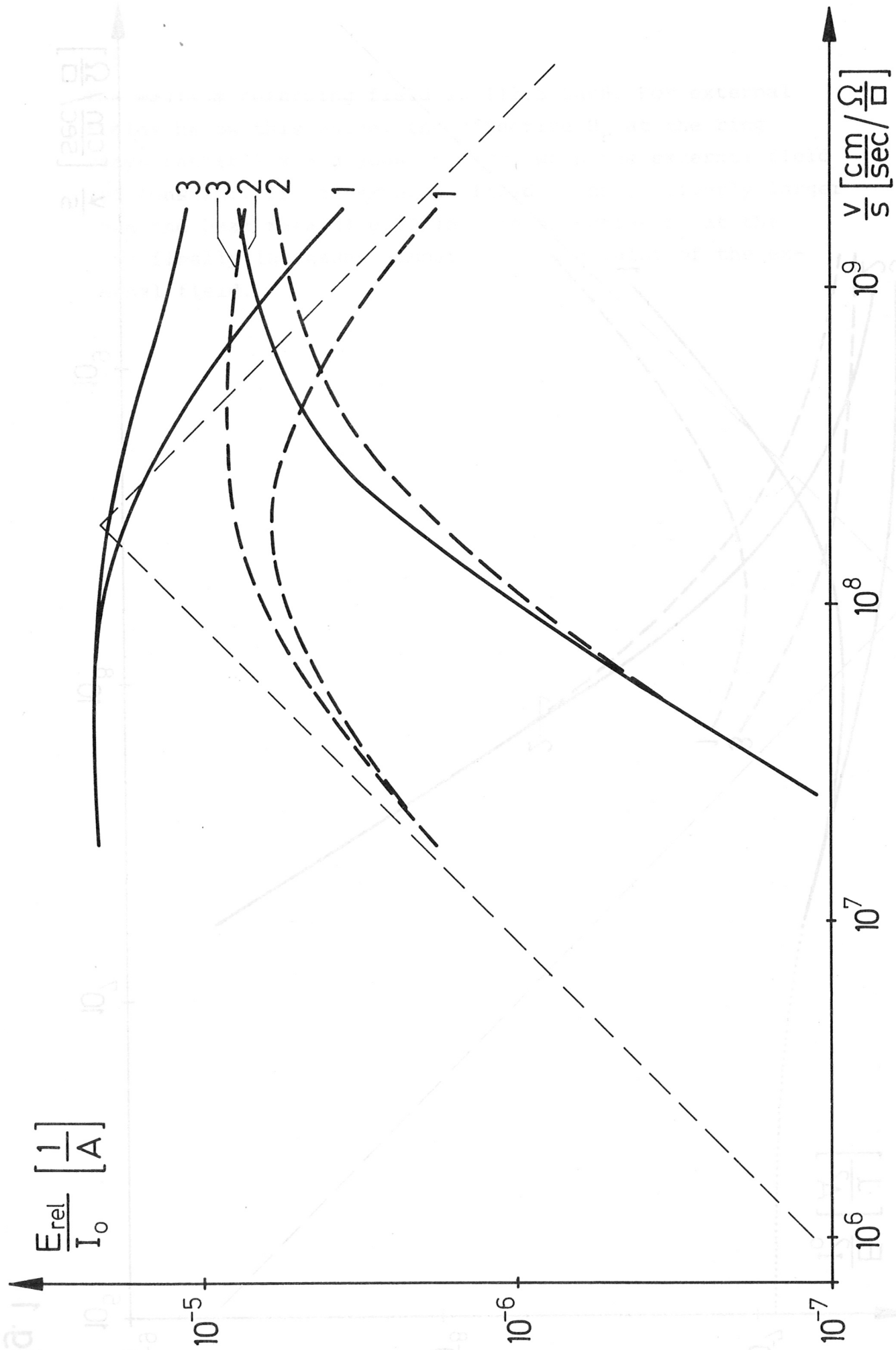


Fig.2

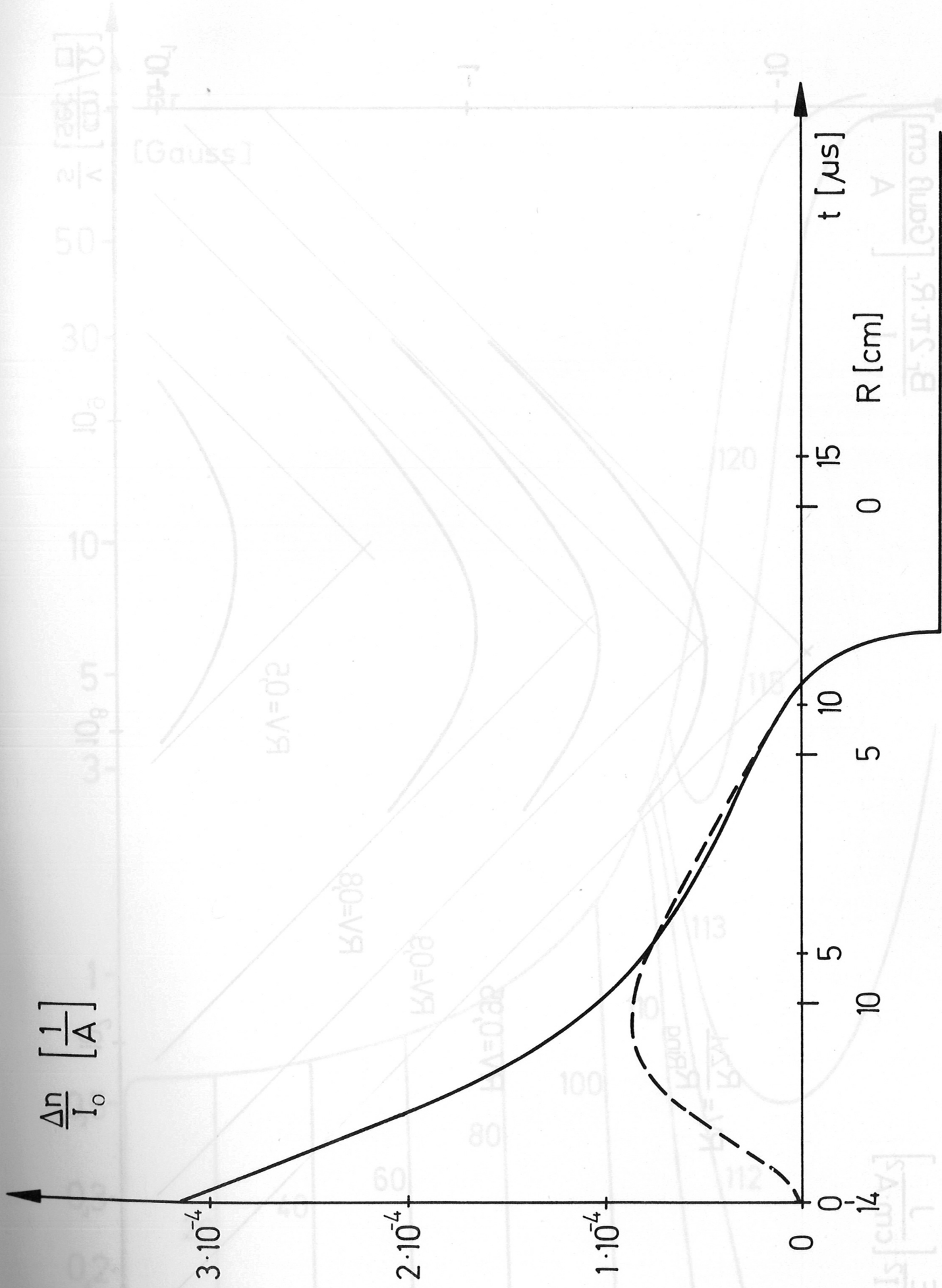


Fig. 3

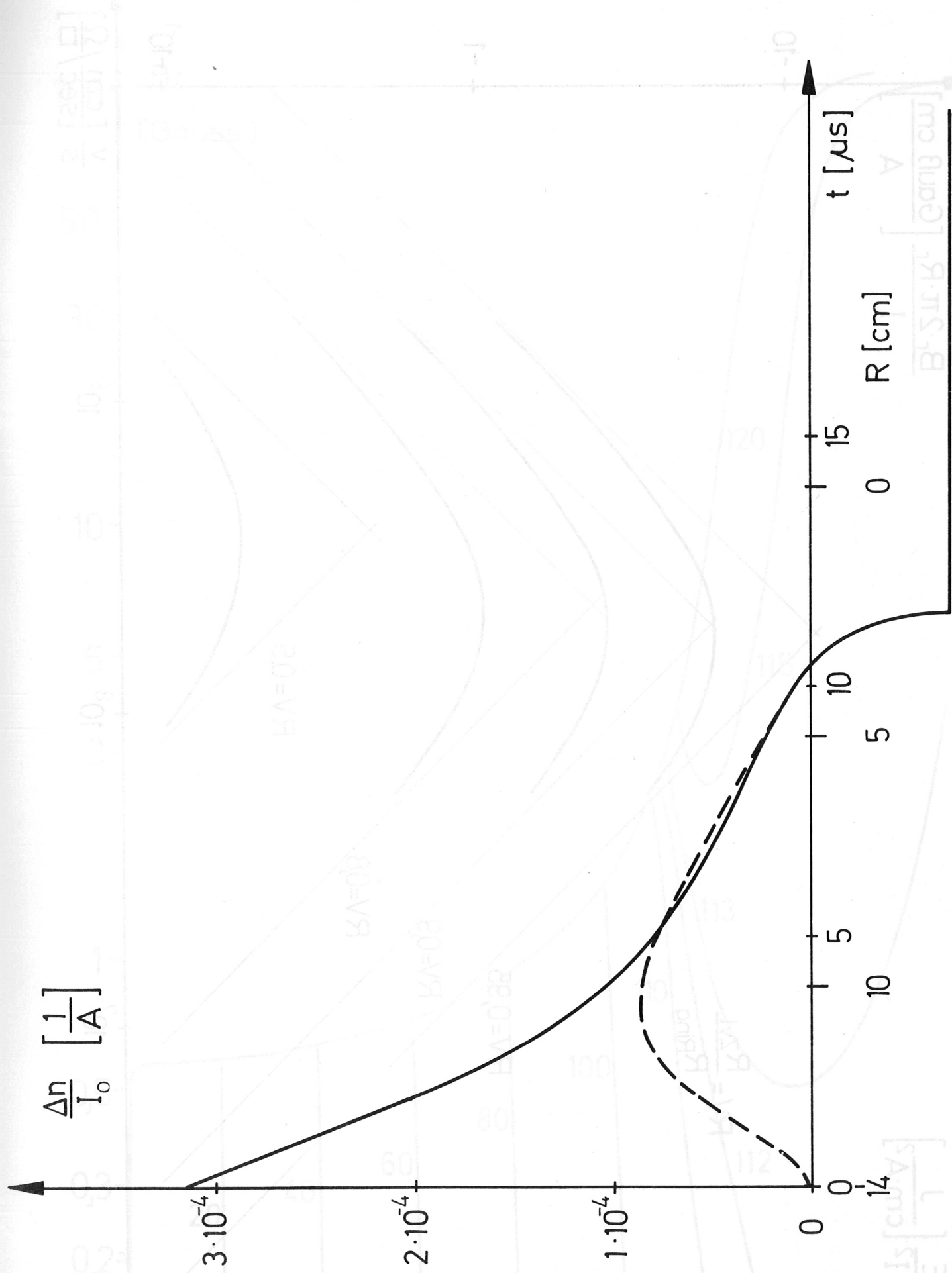


Fig. 3

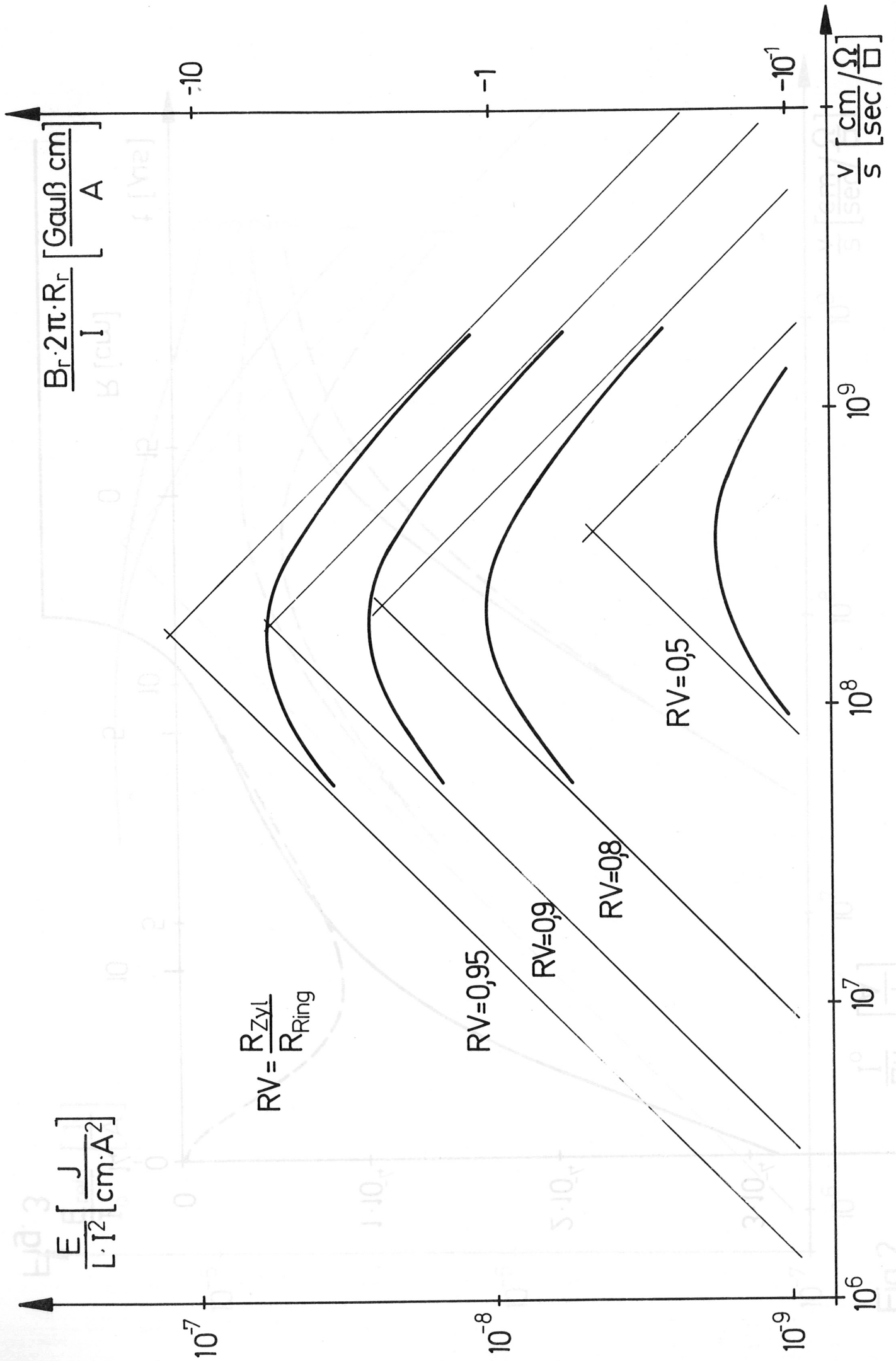


Fig. 4

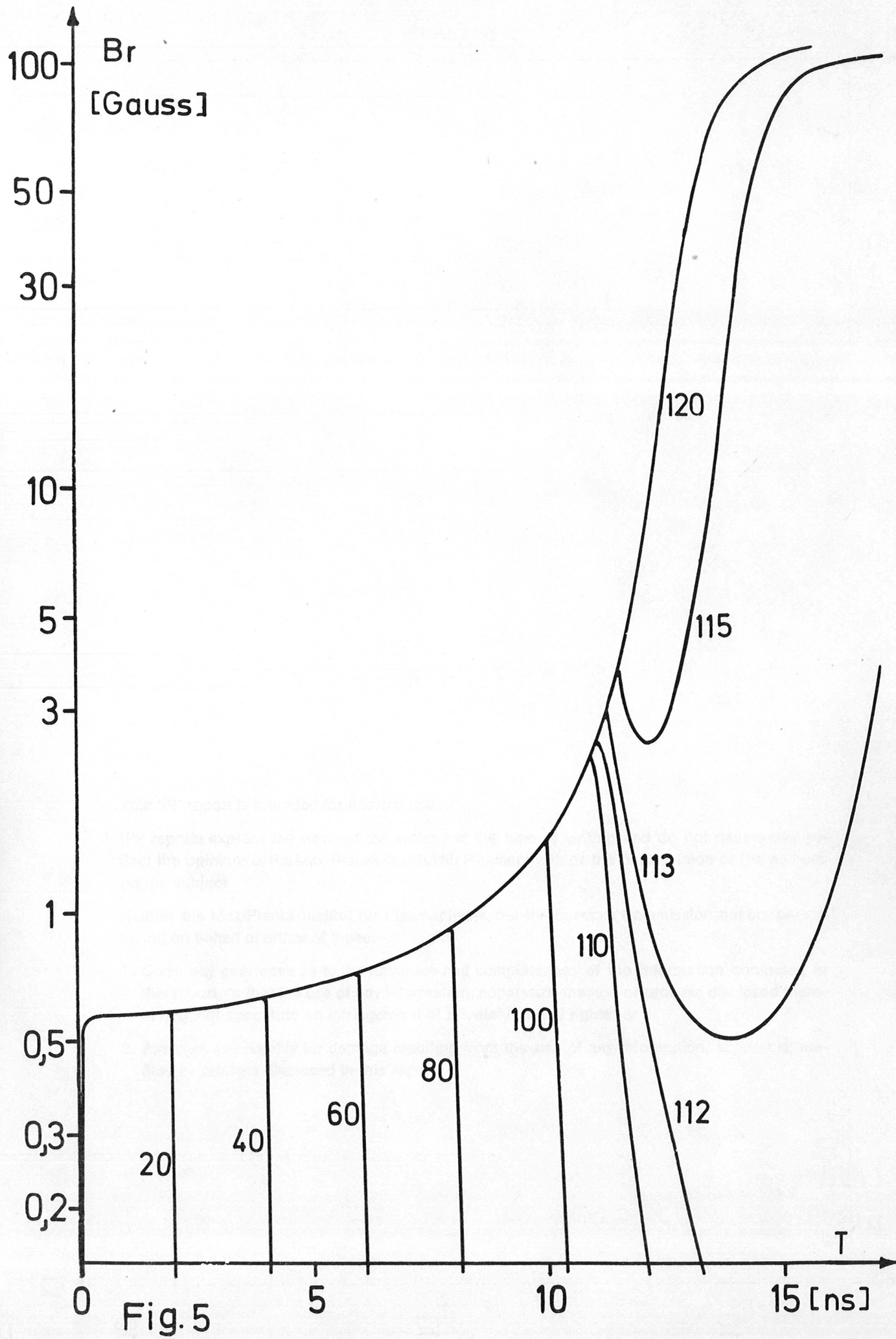


Fig. 5